Boron Monolayers

Deutsche Ausgabe: DOI: 10.1002/ange.201505425
Internationale Ausgabe: DOI: 10.1002/anie.201505425

Two-Dimensional Boron Monolayers Mediated by Metal Substrates

*Zhuhua Zhang, Yang Yang, Guoying Gao, and Boris I. Yakobson**

Abstract: *Two-dimensional (2D) materials, such as graphene and boron nitride, have specific lattice structures independent of external conditions. In contrast, the structure of 2D boron sensitively depends on metal substrate, as we show herein using the cluster expansion method and a newly developed surface structure-search method, both based on first-principles calculations. The preferred 2D boron on weaker interacting Au is nonplanar with significant buckling and numerous polymorphs as in vacuum, whereas on more reactive Ag, Cu, and Ni, the polymorphic energy degeneracy is lifted and a particular planar structure is found to be most stable. We also show that a layer composed of icosahedral B_{12} is unfavorable on Cu and Ni but unexpectedly becomes a possible minimum on Au and Ag. The substrate-dependent 2D boron choices originate from a competition between the strain energy of buckling and chemical energy of electronic hybridization between boron and metal.*

Boron is one of the most intriguing elements not only because of its position between metals and nonmetals in periodic table but also because of its ability to form an enormous number of allotropes.[1] Apart from several bulk (3D) phases,[2] boron can form 0D clusters,[3] 1D nanotubes[4] and nanowires,[5] and 2D layers.[6] In particular, boron sheets of monoatomic thickness have raised interest as a potential new 2D-material and as a (conceptual) precursor, for example, so-called α-sheets,[7] from which other boron structures—fullerene cages[8] and tubes[9]—might be constructed. In fact, a number of planar B clusters up to tens of atoms, found in experiments,[3f–h,k,10] appear as seeds for extended sheets. The 2D boron is shown to be polymorphic,[11] with numerous local minima in a narrow energy interval above the ground line, in contrast to other 2D materials. Boron sheets are rich in multicenter bonding as a result of the electron deficiency of B atoms,[12] making their structures fluxional, unlike for sp^2-bonded 2D materials.[13] These features render the synthesis of 2D boron challenging.

Synthesis of 2D materials is commonly achieved through chemical vapor deposition (CVD) on a metal substrate which catalyzes the reactions and supports the sample,[14] as exemplified by graphene and *h*-BN sheets. In this respect, the 2D B should not be an exception—it must form on a substrate first and then be separated by a transfer process. How and to which extent the 2D B structures are predetermined by metal substrates is important for their synthesis, yet this connection remains elusive. Previous work has probed the nucleation of B clusters on metals,[15] showing that planar clusters are preferred over 3D structures owing to lower nucleation barriers and thus suggesting the possibility of synthesizing 2D B on metals. Therefore, it is important to know what structures will be favored on metals and what interaction dominates at the boron–substrate interface.

The ground-state configurations of freestanding 2D B have been intensively studied by different global minima search methods.[6a,11,16] Including the substrates into such search by most methods will make the computations daunting. As a powerful tool for evaluating the stability of alloys, cluster expansion (CE) method[17] has recently been invoked to explore the stability of various 2D materials.[11,18] Herein, we go one step further, using the CE to explore the structural diversity and stability of 2D B on metals. The systems are treated as a binary "alloy" composed of triangular B sublattices with hexagon vacancies, all on a metal support. We apply the CE method to such alloy systems, which enables a systematic first-principles study of diverse B sheets on common metal substrates, including Au, Ag, and Cu which do not form boride, and on Ni that does. The results are entirely different from other 2D materials and also from freestanding 2D B.

Graphene and *h*-BN exclusively adopt a honeycomb lattice independent of substrate, while 2D MoS_2 shows a little variability yet exists dominantly in a 2H phase. We show herein that 2D B is the first 2D material that does not have its own fixed structure but depends on the metal substrate. On weakly interacting Au, 2D B remains polymorphic as in vacuum but exhibits off-plane buckling. In contrast, on Ag, Cu, and Ni with increased reactivity the configuration energy degeneracy could be lifted, and a specific planar structure is increasingly favored, most likely to emerge from CVD synthesis. Interplay between the 2D B buckling and boron–metal hybridization appears to control the preferred structure of 2D B on metals. A tentative yet intriguing observation worth mentioning is that the adhesion to metals may even turn the 2D B into promising catalyst for the hydrogen-evolution reaction.

The 2D B sheet can be viewed as a triangular lattice (B) with a pattern of vacancies (denoted as □) and formally treated as an alloy $B_{1-v}\square_v$;[11] the vacancy concentration is $v = m/N$, where m is their number in a supercell of N lattice sites.[7] The substrate and sublattice of honeycomb boron framework are configurationally inactive, but each triangular sublattice site (the hexagon center) can be either a B atom or vacancy (Figure 1 a). The commensurability between the B sheets and metal (111) surfaces is met by 0.8–2.5% compression/stretching of the metal lattice. The rhombic 2×2 and rectangular $2\times2\sqrt{3}$ supercells (see the inset in Figure 1 a)

[*] Dr. Z. Zhang, Y. Yang, G. Gao, Prof. B. I. Yakobson
Department of Materials Science and NanoEngineering
Department of Chemistry, and the Smalley Institute
Rice University
Houston, TX 77005 (USA)
E-mail: biy@rice.edu

Supporting information for this article is available on the WWW under http://dx.doi.org/10.1002/anie.201505425.

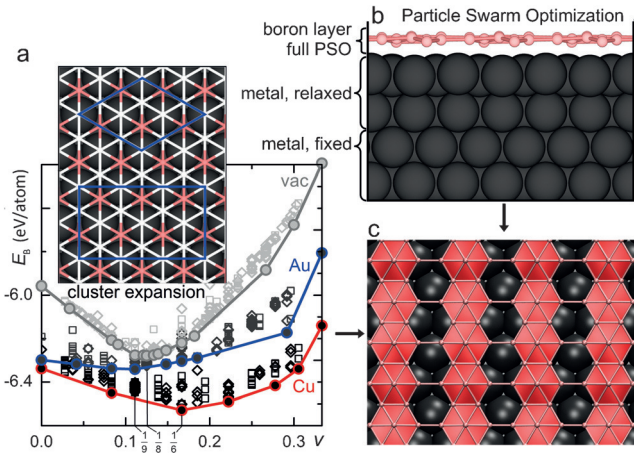

Figure 1. a) Total energy per atom of all symmetry-inequivalent B sheets calculated by CE-fits in vacuum, on Au and on Cu as a function of vacancy concentration v in the $B_{1-v}\square_v$ systems. The solid lines with circles represent the profiles of ground states from precise DFT calculations. Diamonds show the data expanded from a rhombus cell while squares show those expanded from a rectangular cell as illustrated in the inset, where the B sublattice that can be either filled or empty is shown in pink and the configurationally inactive sublattice plus metal is shown in gray. b) The slab model used for particle swarm optimization (PSO), which consists of three regions: the fixed and relaxed metal, and the optimized B layer. c) Predicted ground-state structures of 2D B on Ag or Cu from CE and PSO methods agree with each other.

are initially employed and then also larger supercells are screened, up to 42 B atoms. We use ATAT (alloy theoretical automated toolkit)[19] incorporated with DFT-computed values to extract the energy of all generated structures. More details on the CE and DFT methods[20] are provided in Supporting Information. The stability of various 2D B sheets can be compared in terms of their total energy per atom, defined as $E_B = (E_{syst} - E_{metal})/N_B$, where E_{syst} and E_{metal} are total energies of the boron–metal system and the metal substrate within the same supercell, respectively, and N_B is the number of B atoms. Among ≥ 300 B structures obtained on each metal, we select 30 structures with the lowest E_B for more precise energy calculations.

The CE method restricts the B sheets to a honeycomb lattice, excludes trying non-hexagons and other possible deviations, and thus may miss the true ground state. We hence perform an additional structural search using a newly developed surface reconstruction prediction method[21] based on particle swarm optimization (PSO), as implemented in CALYPSO code,[22] which has no lattice restriction. To predict the 2D B sheets on metals, we set up a metal (111) substrate, generate 2D B structures with various symmetries on it and then relax all the B atoms plus the metal atoms of the topmost two layers using DFT calculations, as illustrated in Figure 1b. Other details about the structural search can be found in the Supporting Information. Testing with Ag and Cu, the PSO-predicted ground-state structures are in good agreement with the CE results (Figure 1c and Figure S1). As the CE method is computationally more effective, we focus on using CE.

We start our discussion by showing the CE results for freestanding 2D B. Figure 1a presents E_B of all symmetry-inequivalent structures calculated by CE fits. The ground states for freestanding 2D B lie within $v = 0.1$–0.14, including not only the previously reported α-, $v_{1/8}$-, $v_{2/15}$-sheets[11] but also a new $v_{4/33}$-sheet. All the sheets are planar, with a buckling of less than 0.2 Å. The energy difference of these structures is within 8 meV/atom, and the $v_{4/33}$-sheet is almost as stable as the $v_{1/8}$-sheet (Figure 2). We are aware that using hybrid functional, such as PBE0,[23] may slightly change the energy difference between the structures[16b] but will not qualitatively affect the conclusions.

The results become totally different on metals. On Au, the CE-predicted ground state of 2D B is found at $v = 1/9$ (Figure 1a), while the second and third stable structures appear at $v = 1/12$. The $v_{1/9}$-sheet is more stable than the two $v_{1/12}$-sheets by only 3 and 6.2 meV/atom, respectively, suggesting that the 2D B on Au remains polymorphic. This assumption is also supported by the glasslike configurational energy spectrum, which displays a great many local minima within an energy window of 10 meV above the ground line (Figure 2). The adhesive energy of the $v_{1/9}$-sheet on Au is 77 meV/atom. Despite such a weak interaction with substrate, the preferred sheets are largely buckled (Figure 2, insets), with a magnitude

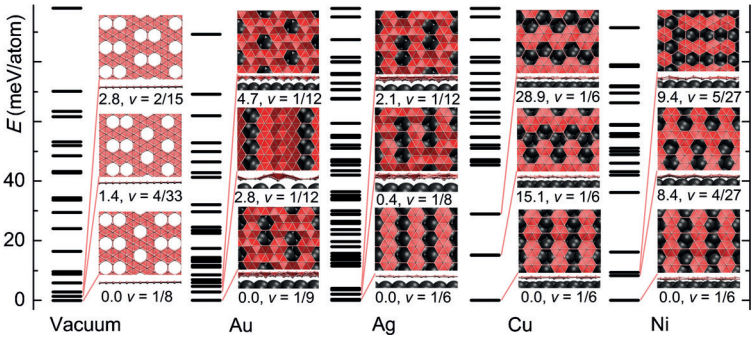

Figure 2. Configurational energy spectra of 2D B in freestanding state, on Au, Ag, Cu, and Ni. The inset in each column illustrates the three most stable structures. Energy with respect to the ground states and the corresponding v are provided below each inset. The B atoms pink, metal atoms black spheres.

of up to 1.1 Å. The $v_{1/9}$-sheet has all the vacancies twinned and evenly dispersed, different from the α-sheet[7] (also $v = 1/9$) that becomes 59 meV/atom less stable on Au.

On Cu, all three sheets with lowest E_B appear at $v = 1/6$ (Figure 1a) and the energy difference between the most and second stable structures is up to 15 meV/atom. The α-sheet is also reproduced but is at 75 meV/atom above the ground line. The three most stable sheets on Cu are rather flat, with undulations of less than 0.3 Å (Figure 2, insets). We name the most stable B sheet as $v_{1/6}$-sheet, which has *Pmmm* symmetry and whose adhesive energy on Cu is 290 meV/atom. The

configurational energy spectrum (Figure 2) at the low energies is much sparser than on Au and in vacuum. Especially, there is a large energy interval of 35 meV/atom, in which only the three most stable sheets fall. Thus, there is a strong driving force towards the formation of specific planar 2D B sheets on Cu. Control of the growth conditions may even enable exclusive formation of the $\nu_{1/6}$-sheet.

For broader picture, we extend our search onto Ag and Ni substrates. The 2D B on Ag is similar to that on Au in terms of the structural buckling and polymorphism (Figure 2). However, the planar $\nu_{1/6}$-sheet on Ag is almost isoenergetic to a buckled structure at $\nu = 1/8$. In contrast, the results on Ni are similar to those on Cu: The low-energy structures are found rather planar and the $\nu_{1/6}$-sheet is distinctly more stable than other structures by at least 8.4 meV/atom. However, structural buckling of the $\nu_{1/6}$-sheet is increased to 0.48 Å by the high reactivity of Ni that results in strong adhesion to the 2D B (Figure S2). These results lead us to conclude that reactive metals outperform inert ones in the possible synthesis of planar 2D B and that the moderately reactive Cu stands out, favoring the flat sheet at the deeper minimum. This important information was missing in previous attempts of structure determination,[15,24] when the 2D B structures were simply guessed or picked from those reported earlier, and are notably less stable than those obtained by comprehensive structural search in present work.

Having determined the preferred structures of 2D B on metals, we proceed to reveal the underlying mechanism of metal-dependent structures. We first consider charge transfer between boron and metal. For 2D B in vacuum, the triangular sublattices act as "donors" while the hexagon vacancies act as "acceptors", which are mixed in a way to compensate the electron deficiency of boron.[7] Extra electrons transferred to the substrate should increase the number of "donors" and result in a B sheet with lower ν. In this sense, the metal work function, which determines boron–metal charge transfer, should be a quantity dominating the substrate effect. However, the result (Figure 3a, solid line) suggests that this is not the case. There is no obvious dependence of the optimal ν on the metal work function. Only when the boron–metal distance is increased (artificially) to approximately 5 Å does the dependence follow the expected decrease (Figure 3a, dashed line). This clearly shows that not the electron transfer but rather chemical hybridization at the boron–metal interface guides the structure choice of 2D B, as analyzed below.

Figure 3b,c present interface charge redistribution of the preferred B-sheets on Au and Cu. Both systems show significant rearrangement of the charge density. The notable electron accumulation in the interface region illustrates the formation of chemical bonding between the boron and the metal. This situation is unusual for Au, least reactive towards adsorbates.[25] Scrutinizing the plots shows a large difference. The charge rearrangement occurs uniformly for all atoms of the $\nu_{1/6}$-sheet on Cu but is highly concentrated on those closer to the metal in the $\nu_{1/9}$-sheet on Au. Interestingly, this charge rearrangement becomes much weaker for a $\nu_{1/6}$-sheet or a flattened $\nu_{1/9}$-sheet on Au (Figure S3a). Therefore, the structural buckling of 2D B on Au is essential: it appears to activate the sheet and enhance the chemical interaction with

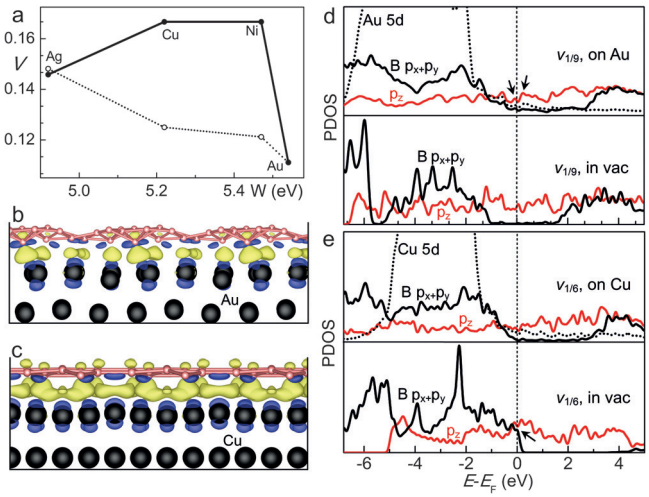

Figure 3. Mechanism of metal dependence of 2D B structures. a) Vacancy concentration ν of ground-state B sheet as a function of the metal work function W. The dotted line is when the boron–metal distance is fixed at 5 Å. Isosurface plots (0.005 e Å^3) of charge redistribution (b) between the $\nu_{1/9}$-sheet and Au as well as c) between the $\nu_{1/6}$-sheet and Cu. Yellow indicates electron accumulation and blue indicates electron depletion. Projected density of states (PDOS) of the d) $\nu_{1/9}$ sheet on Au and e) $\nu_{1/6}$-sheet on Cu, together with the corresponding B sheets in vacuum. The Cu and Au projections are rescaled for clarity.

the inert metal. To shed light on this point, we express the energy E_B of a 2D B sheet on metal as [Eq. (1)]

$$E_B = E_{flat} + E_{bk} + E_{chem} \quad (1)$$

where E_{flat} is the energy per atom of a purely flat B sheet, E_{bk} is the energy change per atom induced by structural buckling, and E_{chem} is the chemical energy averaged onto each B atom by the boron–metal bonding. These energy terms for the $\nu_{1/6}$-sheet on Cu and the $\nu_{1/9}$-sheet on Au are listed in Table 1, together with those for the $\nu_{1/6}$-sheet on Au and the $\nu_{1/9}$-sheet on Cu. Indeed, on Au, the buckled $\nu_{1/9}$-sheet has distinctly higher E_{chem} than the flat $\nu_{1/6}$-sheet does. Moreover, generating large structural buckling is more operable in a B sheet with small ν because of its electron excess.[26] The two reasons explain why the B sheet on inert metal is prone to buckling at relatively small ν. The result is opposite on Cu: The structural buckling of 2D B now reduces E_{chem} because fewer B atoms will effectively interact with the metal (Figure S3b for a $\nu_{1/9\text{-I}}$-

Table 1: Energy decomposition of 2D B on metals.[a]

2D B		E_{flat}	E_{bk}	E_{chem}	E_B	E_{adh}
on Au	$\nu_{1/9}$	−6.221	0.089	−0.197	−6.337	−0.077
	$\nu_{1/6}$	−6.257	0.022	−0.104	−6.302	−0.080
on Cu	$\nu_{1/9\text{-I}}$	−6.249	0.099	−0.288	−6.431	−0.181
	$\nu_{1/6}$	−6.228	0.034	−0.329	−6.521	−0.293

[a] E_{flat}, E_{bk}, E_{chem} are the energies of a purely flat sheet, structural buckling and interfacial bonding, respectively. E_B and E_{adh} are the total and adhesive energies of a B sheet on metal. All the data are given in units of eV/atom. The $\nu_{1/9\text{-I}}$ (see Figure S3b) denotes a different structure from the $\nu_{1/9}$.

sheet on Cu). The B sheet would rather be planar so that all atoms can participate in the interface hybridization, which increases the optimal v. The structure of $\nu_{1/6}$-sheet particularly matches the surface atomic pattern of Cu (111), resulting in a deep global minimum.

To gain deeper insight into the stability of 2D B sheets on metals, we look into the electronic structure. Figure 3d,e present the projected density of states (PDOS) of the preferred $\nu_{1/6}$-sheet on Cu and the $\nu_{1/9}$-sheet on Au, together with the results of corresponding freestanding sheets. For a freestanding $\nu_{1/9}$ sheet, the Fermi level falls in the gap defined by the highest bonding and lowest antibonding states derived from in-plane orbitals ($p_x + p_y$) and cuts the out-of-plane orbitals (p_z), consistent with earlier analysis[27] for the α-sheet. On Au, the structural buckling in the $\nu_{1/9}$ sheet mixes the $p_x + p_y$ and p_z orbitals, extending the $p_x + p_y$ orbital over the whole energy window. As a result, not only the B p_z but also the $p_x + p_y$ orbitals participate considerably in hybridizing with the Au 5d orbitals (predominately $5d_{xy} + 5d_{z^2}$), as evidenced by two resonance peaks in the vicinity of the Fermi level (marked by arrows in Figure 3d). The interfacial bonding is therefore much stronger than that of a planar B sheet on Au (for a planar sheet, the hybridization is solely between the B p_z and Au 5d, see Figure S4). On Cu, the preferred $\nu_{1/6}$-sheet is planar and the interfacial hybridization is predominantly contributed by the B p_z and Cu 5d. Different is that the Cu 5d locates closer to the Fermi level than the Au 5d does and overlaps more substantially with the B p_z orbital. Therefore, the boron–Cu bonding is strong enough to suppress the buckling of the sheet. Moreover, the highest in-plane bonding state is partially occupied for the $\nu_{1/6}$-sheet in vacuum (arrow in Figure 3e) but becomes fully occupied on Cu, implying that boron–Cu charge transfer also contributes in part to stabilize the sheet.

As a conceivable contender to prepare the monolayer 2D B, we also examine the possibility of 2D B_{12} layers because the B_{12} cluster is a unit prevalent in bulk α-boron.[27] In vacuum, the most favorable B_{12} layer is 102 meV/atom less stable than the α-sheet (Figure 4a). On Au and Ag, the B_{12} layer becomes even more stable than the CE-predicted $\nu_{1/9}$- and $\nu_{1/6}$-sheets, by 47.6 and 19.8 meV/atom, respectively. The adhesive energy of the B_{12} layer rises to 210 meV/atom on Au and 175 meV/atom on Ag, which once more supports the notion that on weakly interacting metals the nonplanar structure enhances the boron–metal bonding and stabilizes the B layer. In contrast, the B_{12} layer on Cu and Ni remains a relatively high-energy state, being 54 and 190 meV/atom less stable than the $\nu_{1/6}$-sheet, respectively (Figure 4a). Therefore, the growth of planar 2D B sheet could be more favored on Cu and Ni. All the preferred B layers have a relatively high adhesive energy on metals, larger than that for graphene on Ni. Thus, once synthesized, the 2D B will need a special process to separate it from substrates, such as the method of separating silicene from Ag as recently realized.[28]

Strong adhesion to metal, as we see above, enhances the density of states at the Fermi level of 2D B sheet, which should thus be rich in active sites for catalysis. Using the hydrogen-evolution reaction (HER) as a test, we find that on Au and Ni the 2D B sheet (if not poisoned by other species), may serve as catalysts that are competitive with Pt,[29] according to basic Sabatier principle, with the free energy of adsorbed H on the catalyst usually required to be close to that of the product (Figure 4c and Supporting Information, for calculations details). While further detailed study of this aspect is beyond the scope of current report, this seems worth mentioning.

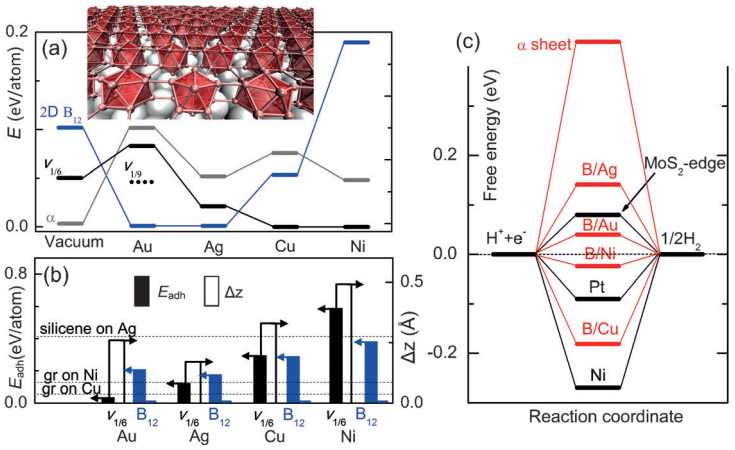

Figure 4. a) Energy order of the α-sheet, $\nu_{1/6}$-sheet, and the B_{12} layer in vacuum and on metals. The reference energy is taken from the most stable structure on each metal. Inset: the atomic configuration of the B_{12} layer on Ag. b) Adhesive energies E_{adh} (filled bars) and buckling Δz (empty bars) of the $\nu_{1/6}$-sheet and 2D B_{12} layer on different metals. E_{adh} for graphene (gr) on Cu and Ni and for silicene on Ag are also provided. c) Free-energy diagram for hydrogen evolution reaction on different catalysts. The free energy of $H^+ + e^-$ is defined as the same as that of $1/2\,H_2$ at room temperature and standard conditions. The results for pure metals and the MoS_2 edge are from Ref. [29].

In summary, we have determined the preferred structures of 2D B on metals by using the cluster-expansion method combined with first-principles calculations, augmented by a newly developed[21] surface structure search based on structure swarm intelligence and free of any grid constraints. In particular, a planar $\nu_{1/6}$-sheet is predicted to be favored on most of the studied metals and must be sought in 2D B growth on metal substrates, calling for experimental tests. The revealed metal-dependent B sheets open a possibility to guide 2D B formation through tailored boron–metal interactions.

Acknowledgements

This work was supported by the Department of Energy, BES Grant DE-SC0001479. We thank Dr. E. S. Penev for useful discussions.

Keywords: boron · density functional calculations · metal substrate · monolayers · 2D materials

How to cite: *Angew. Chem. Int. Ed.* **2015**, *54*, 13022–13026
Angew. Chem. **2015**, *127*, 13214–13218

[1] a) T. Ogitsu, E. Schwegler, G. Galli, *Chem. Rev.* **2013**, *113*, 3425 – 3449; b) B. Albert, H. Hillebrecht, *Angew. Chem. Int. Ed.* **2009**, *48*, 8640 – 8668; *Angew. Chem.* **2009**, *121*, 8794 – 8824.
[2] a) J. He, E. Wu, H. Wang, R. Liu, Y. Tian, *Phys. Rev. Lett.* **2005**, *94*, 015504; b) A. R. Oganov, J. Chen, C. Gatti, Y. Ma, Y. Ma, C. W. Glass, Z. Liu, T. Yu, O. O. Kurakevych, V. L. Solozhenko, *Nature* **2009**, *457*, 863 – 867.
[3] a) D. L. Prasad, E. D. Jemmis, *Phys. Rev. Lett.* **2008**, *100*, 165504; b) T. R. Galeev, C. Romanescu, W. L. Li, L. S. Wang, A. I. Boldyrev, *Angew. Chem. Int. Ed.* **2012**, *51*, 2101 – 2105; *Angew. Chem.* **2012**, *124*, 2143 – 2147; c) H. Li, N. Shao, B. Shang, L.-F. Yuan, J. Yang, X. C. Zeng, *Chem. Commun.* **2010**, *46*, 3878 – 3880; d) L. Wang, J. Zhao, F. Li, Z. Chen, *Chem. Phys. Lett.* **2010**, *501*, 16 – 19; e) J. Zhao, L. Wang, F. Li, Z. Chen, *J. Phys. Chem. A* **2010**, *114*, 9969 – 9972; f) W. Huang, A. P. Sergeeva, H.-J. Zhai, B. B. Averkiev, L.-S. Wang, A. I. Boldyrev, *Nat. Chem.* **2010**, *2*, 202 – 206; g) Z. A. Piazza, H.-S. Hu, W.-L. Li, Y.-F. Zhao, J. Li, L.-S. Wang, *Nat. Commun.* **2014**, *5*, 3113; h) H.-J. Zhai, Y.-F. Zhao, W.-L. Li, Q. Chen, H. Bai, H.-S. Hu, Z. A. Piazza, W.-J. Tian, H.-G. Lu, Y.-B. Wu, *Nat. Chem.* **2014**, *6*, 727 – 731; i) A. P. Sergeeva, I. A. Popov, Z. A. Piazza, W.-L. Li, C. Romanescu, L.-S. Wang, A. I. Boldyrev, *Acc. Chem. Res.* **2014**, *47*, 1349 – 1358; j) E. Oger, N. R. Crawford, R. Kelting, P. Weis, M. M. Kappes, R. Ahlrichs, *Angew. Chem. Int. Ed.* **2007**, *46*, 8503 – 8506; *Angew. Chem.* **2007**, *119*, 8656 – 8659; k) B. Kiran, S. Bulusu, H.-J. Zhai, S. Yoo, X. C. Zeng, L.-S. Wang, *Proc. Natl. Acad. Sci. USA* **2005**, *102*, 961 – 964.
[4] a) D. Ciuparu, R. F. Klie, Y. Zhu, L. Pfefferle, *J. Phys. Chem. B* **2004**, *108*, 3967 – 3969; b) F. Liu, C. Shen, Z. Su, X. Ding, S. Deng, J. Chen, N. Xu, H. Gao, *J. Mater. Chem.* **2010**, *20*, 2197 – 2205; c) V. Bezugly, J. Kunstmann, B. Grundkötter-Stock, T. Frauenheim, T. Niehaus, G. Cuniberti, *ACS Nano* **2011**, *5*, 4997 – 5005; d) J. Tian, Z. Xu, C. Shen, F. Liu, N. Xu, H.-J. Gao, *Nanoscale* **2010**, *2*, 1375 – 1389; e) J. Kunstmann, V. Bezugly, H. Rabbel, M. H. Rümmeli, G. Cuniberti, *Adv. Funct. Mater.* **2014**, *24*, 4127 – 4134.
[5] C. J. Otten, O. R. Lourie, M.-F. Yu, J. M. Cowley, M. J. Dyer, R. S. Ruoff, W. E. Buhro, *J. Am. Chem. Soc.* **2002**, *124*, 4564 – 4565.
[6] a) X. Wu, J. Dai, Y. Zhao, Z. Zhuo, J. Yang, X. C. Zeng, *ACS Nano* **2012**, *6*, 7443 – 7453; b) X. Yang, Y. Ding, J. Ni, *Phys. Rev. B* **2008**, *77*, 041402; c) H. Tang, S. Ismail-Beigi, *Phys. Rev. B* **2010**, *82*, 115412; d) J. Miller, *Phys. Today* **2007**, *60*, 20 – 21; e) X.-F. Zhou, X. Dong, A. R. Oganov, Q. Zhu, Y. Tian, H.-T. Wang, *Phys. Rev. Lett.* **2014**, *112*, 085502.
[7] H. Tang, S. Ismail-Beigi, *Phys. Rev. Lett.* **2007**, *99*, 115501.
[8] a) A. Sadrzadeh, O. V. Pupysheva, A. K. Singh, B. I. Yakobson, *J. Phys. Chem. A* **2008**, *112*, 13679 – 13683; b) N. G. Szwacki, A. Sadrzadeh, B. I. Yakobson, *Phys. Rev. Lett.* **2007**, *98*, 166804; c) X.-Q. Wang, *Phys. Rev. B* **2010**, *82*, 153409.
[9] a) A. K. Singh, A. Sadrzadeh, B. I. Yakobson, *Nano Lett.* **2008**, *8*, 1314 – 1317; b) E. S. Penev, V. I. Artyukhov, F. Ding, B. I. Yakobson, *Adv. Mater.* **2012**, *24*, 4956 – 4976.
[10] a) A. P. Sergeeva, Z. A. Piazza, C. Romanescu, W.-L. Li, A. I. Boldyrev, L.-S. Wang, *J. Am. Chem. Soc.* **2012**, *134*, 18065 – 18073; b) W.-L. Li, C. Romanescu, T. Jian, L.-S. Wang, *J. Am. Chem. Soc.* **2012**, *134*, 13228 – 13231.
[11] E. S. Penev, S. Bhowmick, A. Sadrzadeh, B. I. Yakobson, *Nano Lett.* **2012**, *12*, 2441 – 2445.
[12] T. R. Galeev, Q. Chen, J.-C. Guo, H. Bai, C.-Q. Miao, H.-G. Lu, A. P. Sergeeva, S.-D. Li, A. I. Boldyrev, *Phys. Chem. Chem. Phys.* **2011**, *13*, 11575 – 11578.
[13] M. Evans, J. Joannopoulos, S. Pantelides, *Phys. Rev. B* **2005**, *72*, 045434.
[14] a) X. Zhang, H. Li, F. Ding, *Adv. Mater.* **2014**, *26*, 5488 – 5495; b) A. Reina, X. Jia, J. Ho, D. Nezich, H. Son, V. Bulovic, M. S. Dresselhaus, J. Kong, *Nano Lett.* **2008**, *9*, 30 – 35.
[15] a) Y. Liu, E. S. Penev, B. I. Yakobson, *Angew. Chem. Int. Ed.* **2013**, *52*, 3156 – 3159; *Angew. Chem.* **2013**, *125*, 3238 – 3241; b) H. Liu, J. Gao, J. Zhao, *Sci. Rep.* **2013**, *3*, 3238.
[16] a) X. Yu, L. Li, X.-W. Xu, C.-C. Tang, *J. Phys. Chem. C* **2012**, *116*, 20075 – 20079; b) H. Lu, Y. Mu, H. Bai, Q. Chen, S.-D. Li, *J. Chem. Phys.* **2013**, *138*, 024701.
[17] J. M. Sanchez, F. Ducastelle, D. Gratias, *Physica A* **1984**, *128*, 334 – 350.
[18] a) B. Huang, H. Xiang, Q. Xu, S.-H. Wei, *Phys. Rev. Lett.* **2013**, *110*, 085501; b) A. Kutana, E. S. Penev, B. I. Yakobson, *Nanoscale* **2014**, *6*, 5820 – 5825.
[19] A. Van de Walle, M. Asta, G. Ceder, *CALPHAD Comput. Coupling Phase Diagrams Thermochem* **2002**, *26*, 539 – 553.
[20] a) G. Kresse, J. Hafner, *Phys. Rev. B* **1994**, *49*, 14251; b) G. Kresse, J. Furthmüller, *Phys. Rev. B* **1996**, *54*, 11169.
[21] S. Lu, Y. Wang, H. Liu, M.-s. Miao, Y. Ma, *Nat. Commun.* **2014**, *5*, 3666.
[22] Y. Wang, J. Lv, L. Zhu, Y. Ma, *Phys. Rev. B* **2010**, *82*, 094116.
[23] J. Paier, R. Hirschl, M. Marsman, G. Kresse, *J. Chem. Phys.* **2005**, *122*, 234102.
[24] L. Zhang, Q. Yan, S. Du, G. Su, H.-J. Gao, *J. Phys. Chem. C* **2012**, *116*, 18202 – 18206.
[25] B. Hammer, J. Nørskov, *Nature* **1995**, *376*, 238 – 240.
[26] K. C. Lau, R. Pandey, *J. Phys. Chem. C* **2007**, *111*, 2906 – 2912.
[27] B. Decker, J. Kasper, *Acta Crystallogr.* **1959**, *12*, 503 – 506.
[28] L. Tao, E. Cinquanta, D. Chiappe, C. Grazianetti, M. Fanciulli, M. Dubey, A. Molle, D. Akinwande, *Nat. Nanotechnol.* **2015**, *10*, 227 – 231.
[29] B. Hinnemann, P. G. Moses, J. Bonde, K. P. Jørgensen, J. H. Nielsen, S. Horch, I. Chorkendorff, J. K. Nørskov, *J. Am. Chem. Soc.* **2005**, *127*, 5308 – 5309.

Received: June 15, 2015
Published online: September 2, 2015

